New Journal of Physics
The open-access journal for physics

Ground states of finite spherical Yukawa crystals

H Baumgartner[1], **D Asmus, V Golubnychiy, P Ludwig, H Kählert and M Bonitz**

Institut für Theoretische Physik und Astrophysik,
Christian-Albrechts-Universität, Leibnizstrasse 15,
24118 Kiel, Germany
E-mail: baum@theo-physik.uni-kiel.de

New Journal of Physics **10** (2008) 093019 (18pp)
Received 4 June 2008
Published 15 September 2008
Online at http://www.njp.org/
doi:10.1088/1367-2630/10/9/093019

Abstract. Small three-dimensional strongly coupled clusters of charged particles in a spherical confinement potential arrange themselves in nested concentric shells. If the particles are immersed into a background plasma the interaction is screened. The cluster shell configuration is known to be sensitive to the screening strength. With increased screening, an increased population of the inner shell(s) is observed. Here, we present a detailed analysis of the ground state shell configurations and configuration changes in a wide range of screening parameters for clusters with particle numbers N in the range of 11 to 60. We report three types of anomalous behaviors which are observed upon increase of screening, at fixed N or for an increase of N at fixed screening. The results are obtained by means of extensive first principle molecular dynamics simulations.

[1] Author to whom any correspondence should be addressed.

Contents

1. Introduction

Coulomb crystal formation is among the most exciting cooperative phenomena in charged particle systems and has been observed in a variety of fields, including ultracold ions in Paul and Penning traps [1]–[3], electrons and excitons in semiconductor quantum dots [4] and bilayers [5, 6]. Coulomb crystallization also occurs in classical and quantum two-component systems, such as electron–ion or electron–hole plasmas [7, 8] or laser-cooled expanding plasmas [9], for a recent overview see [10, 11]. Of particular recent interest has been crystallization of charged microspheres in complex plasmas in two dimensions [12]–[14], as well as in three dimensions [15] since here the structure and dynamics of the individual particles is directly visible or recordable by standard CCD cameras, e.g. [16].

From the theoretical side, the shell structure of spherically confined Coulomb crystals has been analyzed in great detail by computer simulations, e.g. [17, 18] and references therein. More accurate data including metastable states have recently been presented [19]–[23] resulting in a very good understanding of these systems. However, in dusty plasmas the interaction of the two particles forming a crystal is screened by the surrounding electrons and ions which has a significant influence on the crystal structure. In [24]–[26] it was shown, by comparison with experiments, that the pair interaction is well described by an isotropic Yukawa potential and shell configurations for various values of the screening strength have been presented. It was found that screening leads to a cluster compression, a change of the average density profile [27, 28] and to an enhanced population of the inner shells. Yet a detailed understanding of how these shell occupation changes proceed is still missing. This is the goal of the present paper.

Here, we present a detailed analysis of the ground state configurations of mesoscopic clusters interacting via an isotropic Yukawa potential containing 11 to 60 particles in a wide range of screening parameters $0.0 \leqslant \kappa \leqslant 20.0$. While the general trend that with increased κ particles move inward is confirmed, we observe several anomalies which are due to symmetry effects: (i) upon κ increase two particles move to the inner shell at once, (ii) when the particle number is increased by one at a fixed κ one particle moves from the inner to the outer shell,

and (iii) at very large κ there exist cases of re-entrent shell fillings: one particle returns from the inner to the outer shell.

2. Model and simulation technique

We consider N identical Yukawa interacting classical particles with mass m and charge q in a three-dimensional isotropic harmonic confinement potential, with the confinement strength α, described by the Hamiltonian

$$H(\mathbf{r}_i, \mathbf{v}_i) = \sum_i^N \frac{m}{2}\mathbf{v}_i^2 + \sum_i^N \frac{\alpha}{2}\mathbf{r}_i^2 + \sum_{ij}^N \frac{q^2}{4\pi\epsilon r_{ij}} \mathrm{e}^{-\kappa r_{ij}}. \tag{1}$$

This model has been found to be close to the experimental situation under which spherical dust crystals form [29]. Deviations from isotropic confinement have been discussed in [25]. In the simulations, we use dimensionless length and energy variables by introducing the units $r_0 = (q^2/16\pi\epsilon\alpha)^{1/3}$ and $E_0 = (\alpha q^4/32\pi^2\epsilon^2)^{1/3}$, respectively.

This model was already used to find the ground state configurations and their energies for Coulomb interaction in [19, 20]. Here, we extended the investigation to the ground states of finite Yukawa systems. To obtain the ground states, we perform extensive molecular dynamics simulation using a standard simulated annealing technique, e.g. [30]. This is done by slowing down the particles by a weak friction coefficient, starting from a random configuration. A stable state is reached when the dimensionless force on each particle is zero (less than 10^{-6} in the calculations). It was observed previously for Coulomb systems that there exist different states with the same shell configuration, which differ with respect to the particle arrangement within the shells (fine structure) [19, 21, 22]. Here, these energy differences which are less than 10^{-8} in dimensionless units will not be resolved since this would blow up the whole analysis and we record only the energetically lowest shell configurations for a given value of κ.

Metastable states with a different shell configuration are sometimes energetically very close to the ground state. Also, their number increases approximately exponentially with N [22], which requires special care in the numerical approach, in particular in the choice of the cooling speed. Also, for given parameters, the cooling process has to be repeated sufficiently often. In the present calculations, we typically used 10^3–10^4 independent runs for every set of (N, κ). While this does not guarantee that the true ground state is found it does ensure a sufficiently high probability that no other state with lower energy exists. As an independent tool to verify the results we performed for a number of cases standard Metropolis Monte Carlo simulations.

We simulated particle numbers from 11 to 60 and screenings from $\kappa = 0$ to $\kappa = 5.0$. The screening parameter was changed in steps of $\Delta\kappa = 0.1$. When for some N a configuration change at some critical κ was detected, the calculation around this point was repeated with a substantial smaller κ step to ensure an accuracy of ± 0.05 in κ at points of structural transitions. The choice of this interval of screening parameters is motivated by the situation of typical dusty plasma experiments where κ is around 1. Besides, what the asymptotic shell configuration will be in the limit of a very short range interaction is of theoretical interest. To this end we also analyzed the ground state at $\kappa = 20$ and recorded structural transitions occurring between $\kappa = 5$ and $\kappa = 20$.

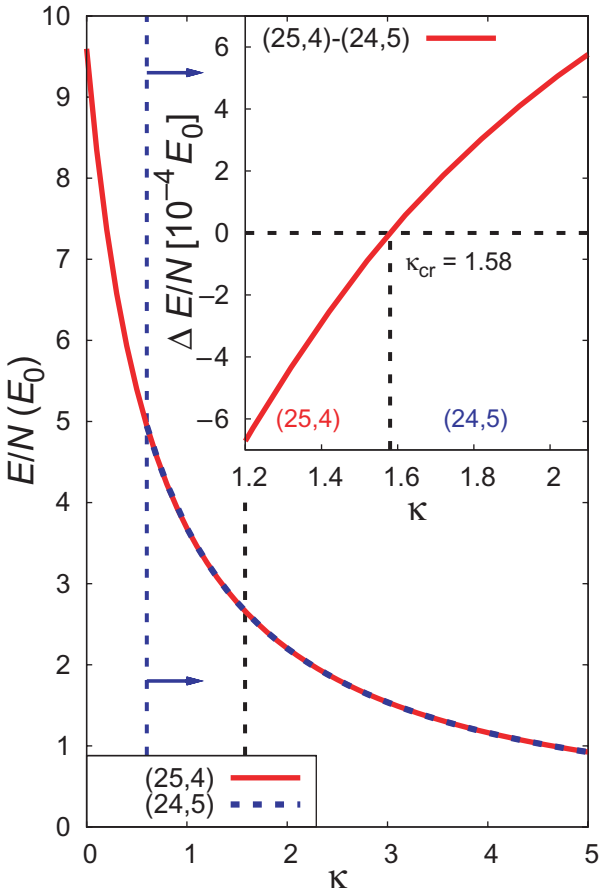

Figure 1. Energy per particle of a Yukawa cluster with $N = 29$ particles for screenings $0.0 \leqslant \kappa \leqslant 5.0$. The red solid [blue dashed] line indicates the configuration $(25, 4)$, [the configuration $(24, 5)$]. The vertical blue dashed line denotes the screening from which the configuration $(24, 5)$ begins to occur in the simulations. The configuration $(25, 4)$ is present in the complete range of screening. The inset shows the energy difference per particle of these two configurations in a small range of screening parameters around the critical value, where the ground state shell configuration changes from $(25, 4)$ to $(24, 5)$. The critical value is indicated by the vertical black dashed line in the inset.

3. Numerical results

3.1. Total energy

A typical simulation result is shown in figure 1, where we plot the total energy per particle for the cluster $N = 29$ in the range of $0.0 \leqslant \kappa \leqslant 5.0$. As one can see the energy decreases rapidly with κ by approximately one order of magnitude, due to the reduction of the pair interaction strength. The same behavior is observed for other particle numbers, as shown for $N = 31$ in figure 2 and, for $N = 57$, in figure 3. Due to the exponential dependence on the distance one may wonder if the energy decrease with κ follows an exponential law as well, as is the case in macroscopic one-component Yukawa plasmas, e.g. [31, 32].

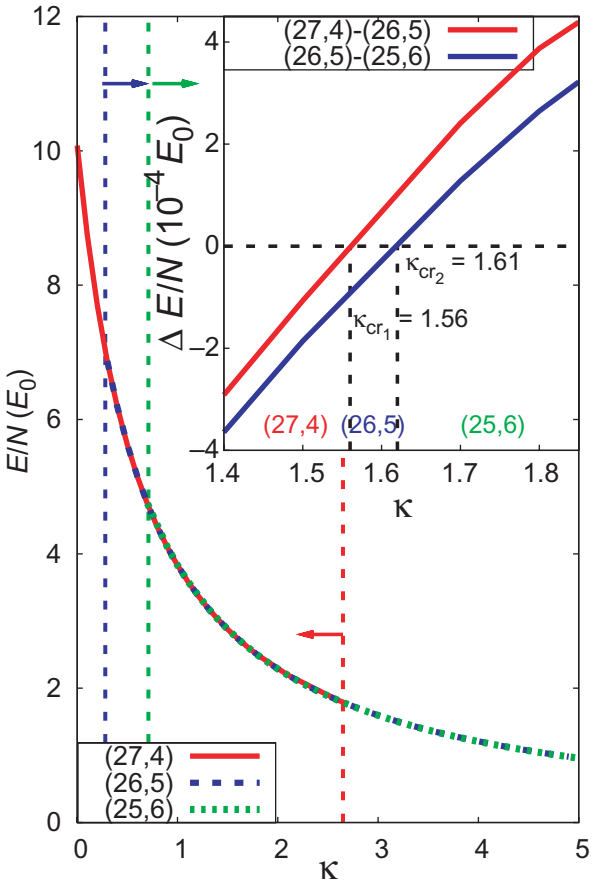

Figure 2. Energy per particle of a Yukawa cluster with 31 particles for screenings $0.0 \leqslant \kappa \leqslant 5.0$. The red solid line indicates the configuration $(27, 4)$ and the blue dashed [green dotted] line the configuration $(26, 5)$ [$(25, 6)$]. The vertical dashed lines denote the beginning [blue for $(26, 5)$ and green for $(25, 6)$] and the end [red for $(27, 4)$] of the occurrence of these configurations in the simulations. The inset shows the energy difference per particle for two stable states: the red [blue] solid line for the configurations $(27, 4)$–$(26, 5)$ [$(26, 5)$–$(25, 6)$] around the critical value of screening. The critical values for the changes in the ground state configurations are indicated by the vertical black dashed lines in the inset.

The simplest fit for the ground state total energy per particle has the form

$$\frac{E^f_{\mathrm{GS}}(\kappa, N)}{N} = E_1(N)\mathrm{e}^{-r_1(N)\kappa} + E_0(N) \tag{2}$$

and uses three κ independent free parameters which are functions of the particle number. In the analyzed range of N this dependence is found to be close to $N^{2/3}$, for the two energies E_0 and E_1, whereas the effective length r_1 in the exponent scales approximately as $N^{1/3}$. Using the exact results for the ground state energies per particle from the molecular dynamics simulations

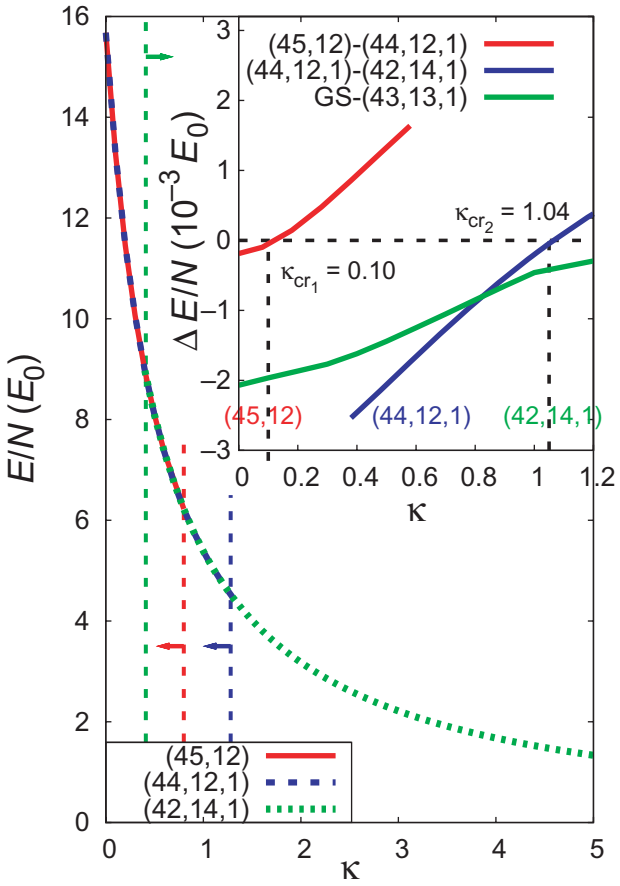

Figure 3. Energy per particle of a Yukawa cluster with 57 particles for screenings $0.0 \leqslant \kappa \leqslant 5.0$. The red solid line indicates the configuration $(45, 12)$ and the blue dashed [green dotted] line the configuration $(44, 12, 1)$ [$(42, 14, 1)$]. The vertical dashed lines denote the beginning [green for $(42, 14, 1)$] and the end [red for $(45, 12)$ and blue for $(44, 12, 1)$, respectively] of occurrence of these configurations in the simulations. The inset shows the energy difference per particle: the red [blue] solid line for the configurations $(45, 12)$–$(44, 12, 1)$ [$(44, 12, 1)$–$(42, 14, 1)$] around the critical range of screening. The green solid line is the energy difference of the metastable configuration $(43, 13, 1)$ to the current ground state, this configuration is never the ground state. The critical values for the changes in the ground state configurations are indicated by the vertical black dashed lines. The change $(44, 12, 1) \rightarrow (42, 14, 1)$ at $\kappa_{cr2} = 1.04$ shows an *anomaly of the first kind*.

we obtain the following best fit for the three coefficients:

$$E_0(N) = 0.015 + 0.12N^{2/3}, \tag{3}$$

$$E_1(N) = -0.81 + 0.92N^{2/3}, \tag{4}$$

$$r_1(N) = 0.51 + 0.19N^{1/3}. \tag{5}$$

Table 1. Ground state energies per particle from equation (3), compared to the exact results from MD simulations, and the relative error Δ, for some examples.

N	κ	E_{GS}/N (MD)	E^f_{GS}/N (equation (3))	Δ (%)
12	0.0	4.839	4.656	−3.8
12	4.0	0.685	0.736	+7.4
58	0.0	15.875	14.788	−6.8
58	4.0	1.692	1.902	+12.4

In the Coulomb limit this fit reduces to

$$\frac{E^f_{GS}(\kappa = 0, N)}{N} = E_0(N) + E_1(N) = -0.795 + 1.04N^{2/3}. \tag{6}$$

This fit is useful to understand the main trends in the analyzed parameter range and reproduces the simulation data within several percent. Some representative examples are given in table 1. Further improvements can be easily achieved using, e.g. the numerical results of [32] or the analytical expressions of [33], but this is outside the goal of the present analysis.

3.2. Structural transitions with screening

The presented fit for ground state total energies E^f_{GS} is a continuous function of κ and does not immediately reveal possible changes of the shell configuration. In fact, in many cases there co-exist several stationary states (shell configurations), the energies of which may become equal at a certain value of κ. At this point a structural transition of the ground state is observed. This can be seen in figure 1 for the cluster with $N = 29$ particles. For small κ the configuration $(25, 4)$ is the ground state until at the critical value of $\kappa_{cr} = 1.58$ the configuration $(24, 5)$ has the same energy and a smaller energy beyond this point, see inset of figure 1. The configuration $(N1, N2)$ means that $N1$ particles are on the first (outer) shell and $N2$ particles are on the second (inner) shell, while shells are counted from outwards to inwards. Thus, if κ crosses κ_{cr} from below, one particle of the cluster moves from the outer to the inner shell. This ground state change is accompanied by a jump of the derivative of the exact ground state energy $dE_{GS}/d\kappa$ at κ_{cr}, so this structural transition resembles a first-order phase transition.

Figure 2 shows a more complicated example with two ground state changes occurring in a small range of screening parameters. For $\kappa < 1.5623$ the ground state configuration is $(27, 4)$, whereas at $\kappa_{cr1} = 1.5623$ the configuration $(26, 5)$ becomes the ground state. Finally, at $\kappa_{cr2} = 1.6142$ this configuration is replaced by $(25, 6)$ which remains the ground state for larger κ. This behavior can be seen in the energy differences plotted in the inset of figure 2. Around the interval $[\kappa_{cr1}, \kappa_{cr2}]$ all three states co-exist and have very close energies which illustrates the high accuracy and fine κ-grid required in this analysis.

These two examples are typical for most cases: at small κ, the cluster structure is strongly influenced by the spherical trap. In contrast, in the limit of very large screening the pair interaction tends to a hard sphere interaction and the clusters approach a closed packed structure. This is often a layered structure allowing for an optimal compression [23]. In between the two limits of long range and short range interaction the shell configurations change via one

(or several) structural transitions where one particle from the outer shell moves to the inner shell as this configuration becomes energetically favorable.

There are, however, several interesting exceptions to this general behavior. We observe three kinds of 'anomalies' which will be analyzed in the following.

3.3. *Anomalies of first kind: correlated two-particle transitions*

Consider now the cluster $N = 57$, cf figure 3. At small screening, the configuration $(45, 12)$ is the ground state until at $\kappa_{\mathrm{cr1}} = 0.10$ one particle from the outer shell moves to the cluster center forming a new shell with the configuration $(44, 12, 1)$. Thereby the second shell is not changed since it has a 'closed shell' configuration with 12 particles. Besides this 'normal' transition, at $\kappa_{\mathrm{cr2}} = 1.04$ a new type of structural change is observed: the configuration changes according to $(44, 12, 1) \rightarrow (42, 14, 1)$. This means, at this point a *correlated intershell transition of two particles* is observed. This unusual behavior will be called an 'anomaly of the first kind'. The reason for this anomaly is the particularly high stability of the closed shell configuration of shell two which dominates the structure up to rather large screening. In contrast, a configuration with 13 particles on the second shell is energetically very unfavorable, although it exists in a broad range of κ values, in fact, the configuration $(45, 13, 1)$ is never the ground state as can be seen in the inset of figure 3.

The first occurrence of an anomaly of the first kind is at $N = 30$, where a transition $(26, 4) \rightarrow (24, 6)$ is observed at $\kappa \approx 1.5$. There is a total of 18 occurrences of such anomalies: at $N = 30, 34, 36, 38, 40, 45$–$54, 57, 58, 60$. The reason for this behavior is that in all the cases but for $N = 57, 58, 60$ the new ground state configuration, e.g. $(24, 6)$ at screening above $\kappa = 1.5$, always forms a platonic body on the inner shell. This is a highly symmetric configuration which obviously decreases the energy per particle better than by just adding one particle [19, 34]. For the cases $N = 30, 34, 36, 38, 40$ the ground state configuration even changes from one platonic body to another, whereas for the cases $N = 46$–54 the system changes from 10 particles on the inner shell to the closed shell configuration with 12 particles.

The only configuration with 11 particles on an inner shell is found for the case $N = 44$, at the very large screening value of $\kappa = 20.0$, which leads to the conclusion that this configuration is energetically unfavorable. In the other three cases, $N = 57, 58, 60$, the ground state configuration changes from $(12, 1)$ to $(14, 1)$ on the inner shells. Although a ground state configuration with $(13, 1)$ particles in the cluster center is observed for some particle numbers in a certain range of screening parameters, the configurations $(12, 1)$ and $(14, 1)$ are far more often the ground state.

These anomalies are shown in the full ground state diagram of figure 4, by the black circles. The complete list is also shown in table 2 by the bold numbers.

3.4. *Anomalies of the second kind: reduction of inner shell population upon increase of N*

Let us now consider changes of the total particle number N at constant screening. The 'normal' trend upon an increase of the particle number by one is, of course, that the new particle is added to one of the existing shells (leaving the other shells unchanged) or moves into the center opening a new shell. However, again, one observes exceptions from this rule, cf figure 4. This effect was already observed for the Coulomb cluster ($\kappa = 0$) with $N = 59$ [19]. It has the ground state configuration $(46, 12, 1)$. Addition of another particle to the cluster gives rise to

IOP Institute of Physics DEUTSCHE PHYSIKALISCHE GESELLSCHAFT

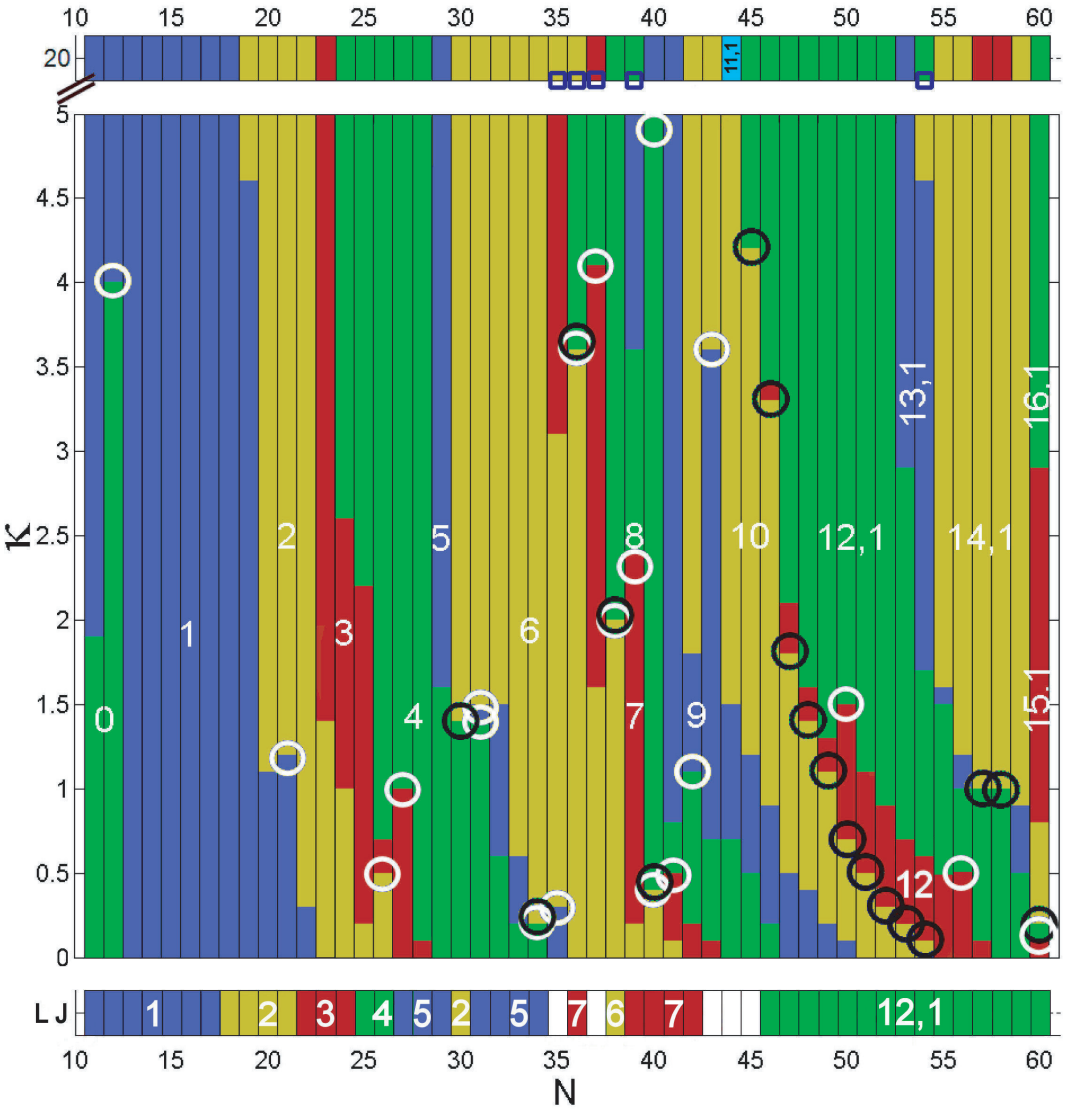

Figure 4. Ground states of small ($11 \leqslant N \leqslant 60$) Yukawa balls for the range of screening parameter ($0.0 \leqslant \kappa \leqslant 5.0$). The numbers on the bars denote the number of particles on the inner shell(s). The black circles indicate anomalies of the first kind. The white circles indicate the end of the screening range, where anomalies of the second kind appear. The ground states for a screening parameter $\kappa = 20.0$ are plotted above the diagram for comparison of in what range the ground states at $\kappa = 5.0$ are stable. The cyan bar for $N = 44$ at $\kappa = 20.0$ refers to a ground state of $(11, 1)$ in the center region; it is the only time this configuration is part of a ground state. The dark blue squares just below $\kappa = 20.0$ indicate anomalies of the third kind, where a ground state configuration reappears with increased screening. Also for comparison the ground state configurations for unconfined Lennard Jones (LJ) clusters are plotted below the diagram, where possible. In the cases $N = 35, 37, 43$–45 (white) it is not possible to define radial shells in the LJ-systems.

Table 2. Table of structural transition points κ_{cr} (cf figure 4). Bold values mark anomalies of the first kind, where the inner shell changes by second particles with increased screening (N fixed). The screening values displayed are the critical values (± 0.05) up to which the configuration given in the third column remains the ground state.

N	κ_{cr}	GS	N	κ_{cr}	GS	N	κ_{cr}	GS	N	κ_{cr}	GS
11	1.9	(11, 0)	**30**	**1.5**	**(26, 4)**	42	0.2	(35, 7)	**51**	**0.5**	**(41, 10)**
	> 5.0	(10, 1)		> 5.0	(24, 6)		1.1	(34, 8)		1.1	(39, 12)
12	4.1	(12, 0)	31	1.56	(27, 4)		1.8	(33, 9)		> 5.0	(38, 12, 1)
	> 5.0	(11, 1)		1.61	(26, 5)		> 5.0	(32, 10)	**52**	**0.3**	**(42, 10)**
13	> 5.0	(12, 1)		> 5.0	(25, 6)	43	0.7	(35, 8)		0.9	(40, 12)
14	> 5.0	(13, 1)	32	0.6	(28, 4)		3.6	(34, 9)		> 5.0	(39, 12, 1)
15	> 5.0	(14, 1)		1.5	(27, 5)		> 5.0	(33, 10)	**53**	**0.2**	**(43, 10)**
16	> 5.0	(15, 1)		> 5.0	(26, 6)	44	0.7	(36, 8)		0.7	(41, 12)
17	> 5.0	(16, 1)	33	0.2	(29, 4)		1.5	(35, 9)		2.9	(40, 12, 1)
18	> 5.0	(17, 1)		0.6	(28, 5)		> 5.0	(34, 10)		> 5.0	(39, 13, 1)
19	4.6	(18, 1)		> 5.0	(27, 6)	**45**	0.5	(37, 8)	**54**	**0.0**	**(44, 10)**
	> 5.0	(17, 2)	**34**	**0.2**	**(30, 4)**		1.2	(36, 9)		0.6	(42, 12)
20	1.1	(19, 1)		> 5.0	(28, 6)		**4.2**	**(35, 10)**		1.7	(41, 12, 1)
	> 5.0	(18, 2)	35	0.3	(30, 5)		> 5.0	(32, 12, 1)		> 5.0	(40, 13, 1)
21	1.2	(20, 1)		3.2	(29, 6)	**46**	0.2	(38, 8)	55	0.5	(43, 12)
	> 5.0	(19, 2)		> 5.0	(28, 7)		0.9	(37, 9)		1.5	(42, 12, 1)
22	0.3	(21, 1)	**36**	**3.6**	**(30, 6)**		**3.3**	**(36, 10)**		1.6	(41, 13, 1)
	> 5.0	(20, 2)		> 5.0	(28, 8)		3.4	(34, 12)		> 5.0	(40, 14, 1)
23	1.4	(21, 2)	37	1.7	(31, 6)		> 5.0	(33, 12, 1)	56	0.5	(44, 12)
	> 5.0	(20, 3)		4.2	(30, 7)	**47**	0.5	(38, 9)		1.0	(43, 12, 1)
24	1.0	(22, 2)		> 5.0	(29, 8)		**1.8**	**(37, 10)**		1.2	(42, 13, 1)
	2.6	(21, 3)	**38**	**2.0**	**(32, 6)**		2.1	(35, 12)		> 5.0	(41, 14, 1)
	> 5.0	(20, 4)		> 5.0	(30, 8)		> 5.0	(34, 12, 1)	**57**	0.1	(45, 12)
25	0.3	(23, 2)	39	0.2	(33, 6)	**48**	0.4	(39, 9)		**1.0**	**(43, 12, 1)**
	2.2	(22, 3)		2.4	(32, 7)		**1.4**	**(38, 10)**		> 5.0	(41, 14, 1)
	> 5.0	(21, 4)		3.6	(31, 8)		1.6	(36, 12)	**58**	**1.0**	**(45, 12, 1)**
26	0.5	(24, 2)		> 5.0	(30, 9)		> 5.0	(35, 12, 1)		> 5.0	(43, 14, 1)
	0.7	(23, 3)	**40**	**0.4**	**(34, 6)**	**49**	0.2	(40, 9)	59	0.5	(46, 12, 1)
	> 5.0	(22, 4)		> 5.0	(32, 8)		**1.1**	**(39, 10)**		0.9	(45, 13, 1)
27	1.0	(24, 3)	41	0.1	(35, 6)		1.4	(37, 12)		> 5.0	(44, 14, 1)
	> 5.0	(23, 4)		0.6	(34, 7)		> 5.0	(36, 12, 1)	**60**	0.1	(48, 12)
28	0.1	(25, 3)		0.8	(33, 8)	**50**	0.1	(41, 9)		**0.2**	**(47, 12, 1)**
	> 5.0	(24, 4)		>5.0	(32, 9)		**0.7**	**(40, 10)**		0.8	(45, 14, 1)
29	1.6	(25, 4)					1.6	(38, 12)		2.9	(44, 15, 1)
	> 5.0	(24, 5)					> 5.0	(37, 12, 1)		> 5.0	(43, 16, 1)

the configuration (48, 12). This is again a structural transition involving correlated behavior of two particles, which we call an 'anomaly of the second kind'. In this particular case, this transition is even associated with a change of the number of shells: the three-shell configuration (first appearing at $N = 58$) disappears again and, instead, a two-shell configuration is restored. This is, of course, a consequence of the particular stability of the latter which contains

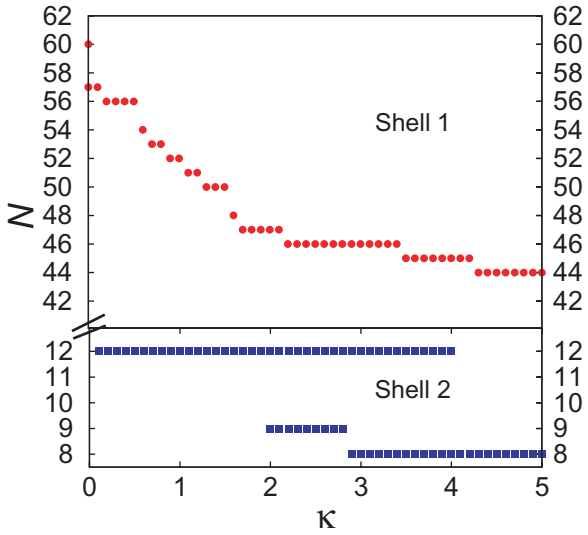

Figure 5. Shell closures for the ground state configurations for the first two shells in the range of screening $0.0 \leqslant \kappa \leqslant 5.0$. The particle number N for the last closed shell is given by red dots (blue squares) for the shell 1 (2) in the considered range of screening. In some cases [$\kappa = 0$ ($2.0 \leqslant \kappa \leqslant 4.0$) for shell 1 (shell 2)] there exist different numbers of particles with closed shells, e.g. $N = 57$ and 60 for $\kappa = 0$.

two closed shells with 12 and 48 particles, respectively. The dependence of the closed shell configurations on the screening is given in figure 5.

While, in Coulomb systems, $N = 59$ is the only known case of an anomaly of the second kind, in Yukawa clusters this behavior appears quite frequently. The first occurrence is at $N = 11$ for κ values between about 2 and 4. Here, addition of a particle gives rise to the configuration change $(10, 1) \rightarrow (12, 0)$, i.e. one particle moves away from the inner shell (the shell vanishes), and the population of the outer shell increases by two. There is a total of 20 such anomalous transitions observed for 18 particle numbers: $N = 11, 20, 25, 26, 30, 33$–$42, 49, 55, 60$. There are two particle numbers where this effect occurs two times: for $N = 30 \rightarrow 31$, in the κ range $[1.5623, 1.6142]$ the configuration changes from $(24, 6)$ to $(26, 5)$. Interestingly, for screening parameters just below this range, i.e. $[1.4866, 1.5623]$ the inner shell even loses two particles, i.e. we observe the transition $(24, 6) \rightarrow (27, 4)$. The second case where two such transitions occur is the transition $39 \rightarrow 40$. There for κ between 0.2223 and 0.4179 the ground state changes according to $(32, 7) \rightarrow (34, 6)$, whereas at $\kappa > 3.612$ the configuration change is $(31, 9) \rightarrow (32, 8)$.

Finally, anomalies of the second kind which are additionally associated with vanishing of one 'shell' (i.e. removal of one particle from the cluster center) are found four times: for $N = 11 \rightarrow 12$ the transition $(10, 1) \rightarrow (12)$ is observed (see above). Return to a two shell configuration occurs three times: for $N = 49 \rightarrow 50$, we find the transition $(36, 12, 1) \rightarrow (38, 12)$, for $N = 55 \rightarrow 56$, the transition $(42, 12, 1) \rightarrow (44, 12)$ and, for $N = 59 \rightarrow 60$, the transition $(46, 12, 1) \rightarrow (48, 12)$, which is known from the Coulomb case (see above) and appears here in a narrow range of small κ values. The complete set of these anomalies is given in table 3.

Table 3. Table of anomalies of the second kind. Left column shows the change of the total particle number by one and column two the associated configuration change. The third and fourth column give the range of screening parameters where this transition occurs.

$N_1 \to N_2$	Configuration	$\kappa_{\min}$	$\kappa_{\max}$
$11 \to 12$	$(10, 1) \to (12)$	1.9038	4.0567
$20 \to 21$	$(18, 2) \to (20, 1)$	1.0762	1.1906
$25 \to 26$	$(22, 3) \to (24, 2)$	0.2544	0.5049
$26 \to 27$	$(22, 4) \to (24, 3)$	0.7287	1.0412
$30 \to 31$	$(24, 6) \to (27, 4)$	1.4866	1.5623
$30 \to 31$	$(24, 6) \to (26, 5)$	1.5623	1.6142
$33 \to 34$	$(28, 5) \to (30, 4)$	0.2012	0.2450
$34 \to 35$	$(28, 6) \to (30, 5)$	0.2450	0.3034
$35 \to 36$	$(28, 7) \to (30, 6)$	3.1665	3.6133
$36 \to 37$	$(28, 8) \to (30, 7)$	3.6133	4.1646
$37 \to 38$	$(30, 7) \to (32, 6)$	1.6679	2.0283
$38 \to 39$	$(30, 8) \to (32, 7)$	2.0283	2.4396
$39 \to 40$	$(32, 7) \to (34, 6)$	0.2223	0.4179
$39 \to 40$	$(31, 9) \to (32, 8)$	3.6120	> 5.0000
$40 \to 41$	$(32, 8) \to (34, 7)$	0.4179	0.5521
$41 \to 42$	$(32, 9) \to (34, 8)$	0.8329	1.1372
$42 \to 43$	$(32, 10) \to (34, 9)$	1.8473	3.6391
$49 \to 50$	$(36, 12, 1) \to (38, 12)$	1.3753	1.5634
$55 \to 56$	$(42, 12, 1) \to (44, 12)$	0.4964	0.5150
$59 \to 60$	$(47, 12, 1) \to (48, 12)$	0.0000	0.1024

3.5. Anomalies of the third kind: re-entrant shell transition upon increase of κ

Finally, there is a the third kind of anomalous behavior which deviates from the 'normal' shell filling trend of increased populations of the inner shells upon increase of κ at a constant N. This tendency is never violated in the considered range of particle numbers, $11 \leqslant N \leqslant 60$, and for $\kappa \leqslant 5$. Since $\kappa = 5$ corresponds to a pair interaction of very short-range one might expect that further increase of κ will not change the cluster structure qualitatively. To verify whether this is the case we performed, for all N, additional calculations for an even larger screening, $\kappa = 20.0$, cf figure 4. In most cases there is, indeed, no further change of the ground state configuration compared to $\kappa = 5$, as expected. For four particle numbers, $N = 40, 44, 57, 58$, the ground state configuration still changes in the 'normal' way such that one particle is relocated from the outer shell to the inner shell.

However, there are six remarkable cases which violate this trend: $N = 35, 36, 37, 39, 54$ and $N = 44$. Consider first the total particle number $N = 44$. This case is interesting because it is the only case where the central configuration $(11, 1)$ is part of the ground state, apart from the cluster with 12 at screenings $\kappa \geqslant 4.1$. This arrangement otherwise does not occur because the clusters prefer the platonic body with 12 particles on the inner shell (closed shell configuration). Here, the configuration $(31, 11, 1)$ becomes the ground state at $\kappa = 17.4$ and remains the ground state for larger screening.

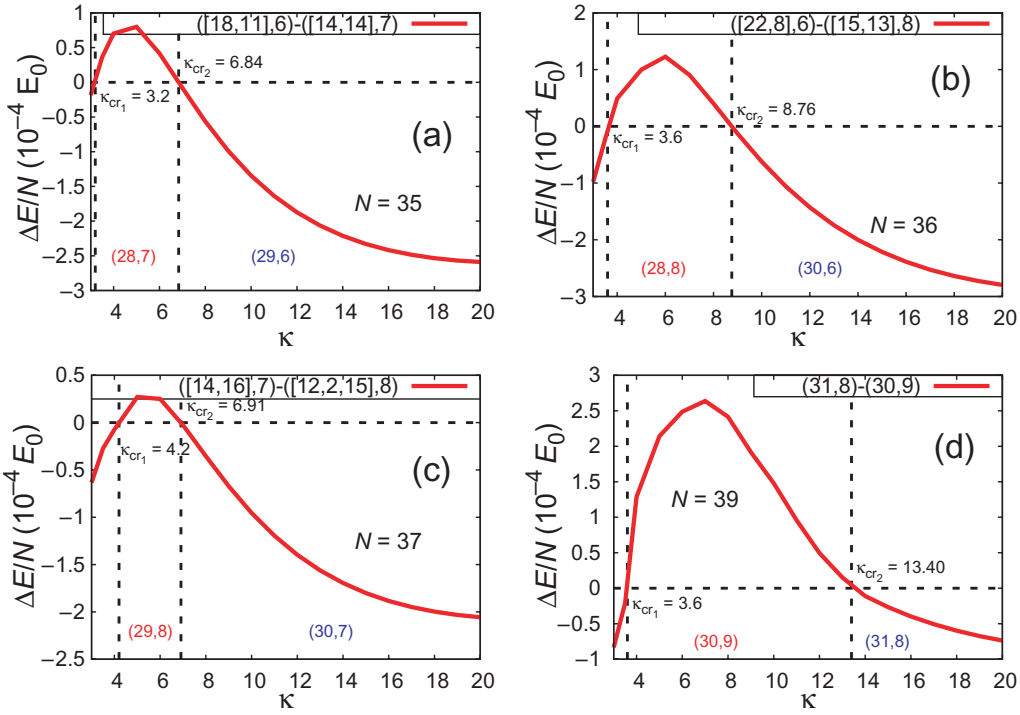

Figure 6. Re-entrant shell configuration changes for $N = 35$ (top left), 36 (top right), 37 (bottom left) and 39 (bottom right). When κ is increased, at κ_{cr1} one particle moves toward the center and, at κ_{cr2}, one particle returns to the outer shell restoring the former ground state configuration. The critical values of κ are indicated by the vertical dashed lines. The solid red line shows the energy difference of the two configurations which has two zeroes. The legend shows the shell configurations, including the splitting of the outer shell into subshells, given by the numbers in square brackets.

In the other five cases we observed, at $\kappa = 20.0$, several stationary states which differed only very little in their energies. We, therefore, performed molecular dynamics simulations using each of these states separately as an input at $\kappa = 20.0$, and then decreased the screening slightly, letting the system relax into a new stationary state, often with the same configuration and symmetry. This way we could be certain to follow all metastable states and independently record their energy dependence on κ. The above five cases fall into two groups which differ with respect to the cluster symmetry. For the first, i.e. $N = 35, 36, 37, 39$, the cluster decreases the number of particles on the inner shell when the screening is increased between $\kappa = 5.0$ and 20.0. The resulting new ground state configuration contains again a platonic body on the inner shell. Allowing for such a highly symmetric configuration here turns out to be energetically more favorable compared to the previous shell configuration or a simple increase of the number of particles on the inner shell.

Consider, for example, the cluster $N = 39$, cf figure 6(d). Here, at $\kappa = 5$ the ground state is $(30, 9)$ until, at $\kappa_{\mathrm{cr}} = 13.40$, the configuration $(31, 8)$ with one particle less on the inner shell becomes the ground state.

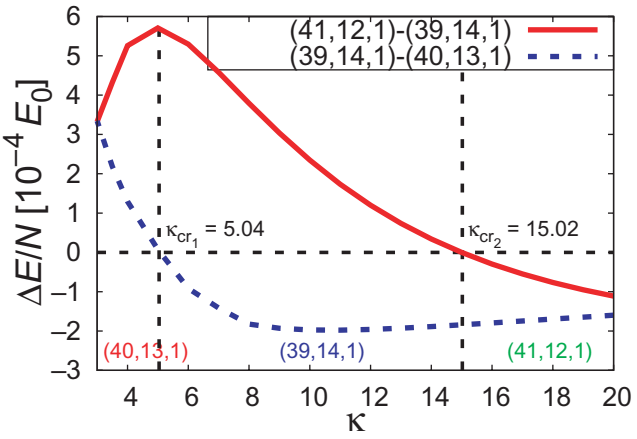

Figure 7. The energy differences of all states which become the ground state in the screening range $4.0 \leqslant \kappa \leqslant 20.0$ for the particle number $N = 54$. In this case, increase of κ leads to a ground state with fewer particles on the second shell, returning to a ground state configuration that already existed at lower screenings. In this case, an 'anomaly of the third kind' is observed.

The particle number reduction on inner shells is sometimes accompanied by another trend: with increasing κ shells tend to split into subshells with close radii, as was already observed in [23, 25]. This is observed, e.g. for $N = 35$, cf figure 6(a). Here the configuration $(28, 7)$ which is the ground state at $\kappa = 5$ has in fact two subshells each containing 14 particles which we will denote $([14, 14], 7)$. The radii of the two subshells differ only slightly, $R_{2,1} = 0.947$ and $R_{2,2} = 0.875$, respectively, whereas the inner shell radius is $R_1 = 0.426$, clearly distinguishable from the outer shell. At $\kappa_{cr} = 6.84$, we observe a transition $([14, 14], 7) \rightarrow ([18, 11], 6)$, i.e. one particle from the inner shell moves outward and, in addition, three particles from the inner subshell move to the outer subshell.

Similar behavior is observed for $N = 36$, cf figure 6(b). Here the configuration $([15, 13], 8)$ is the ground state at $\kappa = 5$. At $\kappa_{cr} = 6.84$, we observe a transition $([15, 13], 8) \rightarrow ([22, 8], 6)$, where the inner shell loses two particles and, in addition, the inner subshell transfers five particles to the outer subshell. Analogously, for $N = 37$, cf figure 6(c), the configuration $([12, 2, 15], 8)$ is the ground state at $\kappa = 5$. At $\kappa_{cr} = 6.91$, we observe a transition $([12, 2, 15], 8) \rightarrow ([14, 16], 7)$, where the inner shell loses one particle.

The cluster with $N = 54$ shows a similar behavior, cf figure 7. Here, first the second shell poplulation increases by one, at $\kappa_{cr1} = 5.04$, according to $(40, 13, 1) \rightarrow (39, 14, 1)$. Further increase of screening makes a third configuration more favorable which has even two particles less on the second shell: the configuration $(41, 12, 1)$ becomes the ground state again at $\kappa_{cr2} = 15.02$, which again is a consequence of the high symmetry (closed shell configuration).

Finally, particularly interesting behavior is observed for all mentioned $N = 35$, $36, 37, 39, 54$, if a larger range of screening is considered, cf figures 6 and 7. Here, for $\kappa \geqslant 1.7$, there are two states which become the ground state. At the first critical value κ_{cr1} one particle moves to the inner shell until at κ_{cr2} this transition is reversed (the only difference for $N = 54$ is that there is an additional ground state configuration between these two critical screenings): one particle moves outward and the original configuration with fewer particles

Table 4. Table of anomalies of the third kind. The first configuration is the ground state configuration up to the critical screening κ_{cr_1}, then the ground state configuration changes in the standard way by adding a particle on an inner shell. This configuration is then the ground state up to the critical screening κ_{cr_2}, at which the cluster changes its ground state configuration back to the one it had at lower screening (*anomaly of the third kind*).

N	Conf. 1	κ_{cr1}	Conf. 2	κ_{cr2}	Conf. 3
35	(29, 6)	3.2	(28, 7)	6.84	(29, 6)
36	(30, 6)	3.6	(29, 7)	8.76	(30, 6)
37	(30, 7)	4.2	(29, 8)	6.91	(30, 7)
39	(31, 8)	3.6	(30, 9)	13.40	(31, 8)
54	(41, 12, 1)	1.68	(40, 13, 1)	5.04	
		5.04	(39, 14, 1)	15.02	(41, 12, 1)

on the inner shell is restored which remains the ground state for all larger values of κ. This contradiction to the general trend (of increasing the inner shell population with increased screening), together with the reappearance of a ground state configuration, will be called an 'anomaly of the third kind'. The complete set of these cases can be found in table 4 with the exact critical screening parameters for the ground state configuration changes. The re-entrance of these ground state configurations at large screening are in all cases not different in their symmetry compared to the ground state configurations below κ_{cr1}, they have the same number of nearest neighbors and the same shape of the Voronoi cells, with only their length scale strongly reduced due to the weaker interaction force.

In general, the restored ground state configurations consist of platonic bodies on the inner shell, except for the case of $N = 37$. Here, the ground state configuration changes from $(30, 7)$ to $(29, 8)$ at a screening value of $\kappa = 4.2$ and back to $(30, 7)$ at a screening value of $\kappa = 6.91$. The seven particles on the inner shell are not a platonic body and, as one can see from figure 4, it is not a common configuration compared to six or eight particles in the center. Nevertheless, this can be understood by looking at the outer shell. The 30 particles are placed on the edges of an icosahedron which results in a highly symmetric configuration for the outer shell.

3.6. Comparison with LJ clusters

The main difference between LJ clusters and Yukawa balls is the nature of the interaction potential. While particles with the purely repulsive Yukawa interaction necessarily require an external confinement to form crystals, this is not true for the LJ potential as it has an attractive tail. The ground states of LJ clusters have been studied extensively and are summarized in [35] for $N \leqslant 110$.

In contrast to Yukawa balls which always have a shell structure, the form of LJ clusters is somewhat different. For most values $N \leqslant 60$ the global minimum consists of a Mackay icosahedron surrounded by a low energy layer of the remaining particles [35]. Closed shells are observed for $N = 13$ and 55 with an icosahedral structure and a particle in the center of the cluster. Compared to Yukawa balls where adding one particle to a closed-shell configuration leads to a new *inner* shell, adding one particle here often gives rise to the onset of a new *outer*

'shell'. This is the reason why the first closed-shell configuration is found for $N = 13$ (LJ)—with a particle in the center, whereas Yukawa balls have their first closed-shell configurations for $N = 12$—without a center particle. The same behavior is found for the second closed-shell configuration with $N = 55$ (LJ), which is not observed for Yukawa balls (cf figure 5).

In figure 4, only the innermost shells of LJ systems are shown where a shell determination was possible. The particles of clusters without closed-shell configurations are not uniformly distributed on the shells. As an example consider the transition $N = 13 \rightarrow 14$. The 14th particle is not added to the first shell but is attached to the surface of the $N = 13$ cluster and forms a new outer 'shell' with an occupation number of one. In the case of Yukawa balls, the additional particle would generally open a new inner shell (center particle) or would be added to one of the existing shells. The positions of the particles on this shell would be changed such that the particles stay as far away from each other as possible, with the strongest tendency for Coulomb interaction and a diminishing effect for larger κ. A single particle on an outer shell is unfavorable due to the symmetry of the trap and the purely repulsive forces. A trend similar to LJ clusters is only observed for very high κ where sub-shells can be found with an occupation number higher than those of nearby outer shells, figure 7. It would be interesting to analyze the effect of an external trap on the structure of LJ clusters without closed-shell configurations to further investigate the influence of a confinement on the emergence of shells as found in Yukawa balls.

4. Conclusions

The goal of this paper was to present, for the first time, a detailed analysis of the ground state shell configurations of Yukawa clusters in a parabolic spherical confinement over a broad range of screening parameters $\kappa \leqslant 20$. This allowed us to analyze the structural transitions occurring when the pair interaction changes from long range, in the Coulomb case, to short range, at the largest values of κ. Focusing on a finite range of particle numbers, $11 \leqslant N \leqslant 60$, we presented a complete overview on all existing changes of the shell configurations for $\kappa \leqslant 5$. For larger κ, we also noted the cases where the configurations are different at $\kappa = 5$ and 20 (we cannot rule out that, in this range, there occur transitions in addition to those given). The general trend observed earlier [24] was confirmed: with increased screening, more particles tend to populate the inner shell(s) of the cluster giving rise to an average density profile which decreases increasingly fast toward the edge [27, 28]. There are, however, three nontrivial deviations ('anomalies') from this shell filling sequence which were analyzed: (i) upon κ increase two particles move to (one of) the inner shell(s) at once, (ii) when the particle number is increased by one, at a fixed κ, one particle moves from the inner to the outer shell, and (iii) at very large κ there exist cases of re-entrent shell fillings: one particle returns from the inner to the outer shell. These anomalies are, in most cases, dictated by symmetry properties of the corresponding state which allow the total energy to be lowered.

Our results are expected to be useful also for experiments with dusty plasmas and allow us to predict interesting parameter ranges, which give information on the effect of symmetry on the structure of mesoscopic systems. In current experiments on spherical dust crystals performed at the Universities of Kiel and Greifswald [15] typical values of the screening parameter are in the range of $0.6 \leqslant \kappa \leqslant 1.6$. While this gives access only to a small part of the analyzed parameters where no re-entrant shell fillings (third anomaly) occur, still the first two effects should be observable. While the experiments on small clusters do not necessarily reveal the ground state configurations, since often metastable states occur with a higher probability

[36, 37] the prediction of parameters where two states have the same energy is of practical interest for the analysis of potential energy barriers and intershell transitions.

Finally, after exploring the shell configuration of small spherical Yukawa clusters it remains to study in detail the geometrical arrangement of particles on the shells. In the case of small Coulomb clusters most particles have either five or six nearest neighbors, e.g. [17]–[19]. Occasional occurrences of four and seven neighbors can be associated with crystal defects, e.g. [22]. For large particle numbers, $N > 1000$, boundary effects and the spherical symmetry caused by the confinement should become gradually less important [38], and the crystal structure should approach that of macroscopic Yukawa crystals which is either of bcc- or fcc-type [31]. How this transition occurs when the particle number is increased and how it changes with the screening strength remain interesting questions. At the same time, it will be interesting to explore how the excitation (normal mode) spectrum, e.g. [39] and references therein, transforms into the phonon spectrum of a macroscopic solid.

Acknowledgments

We thank A Melzer and D Block for stimulating discussions. This work was supported by the Deutsche Forschungsgemeinschaft via SFB-TR 24, grants A5 and A7 and by the US Department of Energy award DE-FG02-07ER54946.

References

[1] Wineland D J *et al* 1987 *Phys. Rev. Lett.* **59** 2935
[2] Drewsen M *et al* 1998 *Phys. Rev. Lett.* **81** 2878
[3] Dubin D H E and O'Neill T M 1999 *Rev. Mod. Phys.* **71** 87
[4] Filinov A, Bonitz M and Lozovik Yu E 2001 *Phys. Rev. Lett.* **86** 3851
Filinov A, Bonitz M and Lozovik Yu E 2000 *Phys. Status. Solidi* b **221** 231
[5] Ludwig P, Filinov A, Bonitz M and Lozovik Yu E 2003 *Contrib. Plasma Phys.* **43** 285–9
[6] Ludwig P, Filinov A, Lozovik Yu, Stolz H and Bonitz M 2007 *Contrib. Plasma Phys.* **47** 335–44
[7] Bonitz M, Filinov V S, Fortov V E, Levashov P R and Fehske H 2005 *Phys. Rev. Lett.* **95** 235006
[8] Bonitz M, Filinov V S, Fortov V E, Levashov P R and Fehske H 2006 *J. Phys. A: Math. Gen.* **39** 4717
[9] Pohl T, Pattard T and Rost J M 2004 *Phys. Rev. Lett.* **92** 155003
[10] Bonitz M *et al* 2008 *Phys. Plasmas* **15** 055704
[11] Morfill G E, Annaratone B M, Bryant P, Ivlev A V, Thomas H M, Zuzic M and Fortov V E 2002 *Plasma Phys. Control. Fusion* **44** B263–77
[12] Chu J H and Lin I 1994 *Phys. Rev. Lett.* **72** 4009
[13] Thomas H, Morfill G E, Demmel V, Goree J, Feuerbacher B and Möhlmann D 1994 *Phys. Rev. Lett.* **73** 652
[14] Fortov V E, Filinov V S, Nefedov A P, Petrov O F, Samaryan A A and Lipaev A M 1996 *J. Exp. Theor. Phys.* **84** 489–96
[15] Arp O, Block D, Piel A and Melzer A 2004 *Phys. Rev. Lett.* **93** 165004
[16] Käding S and Melzer A 2006 *Phys. Plasmas* **13** 090701
[17] Hasse R W and Avilov V V 1991 *Phys. Rev.* A **44** 4506
[18] Tsuruta K and Ichimaru S 1993 *Phys. Rev.* A **48** 1339
[19] Ludwig P, Kosse S and Bonitz M 2005 *Phys. Rev.* E **71** 046403
[20] Arp O, Block D, Bonitz M, Fehske H, Golubnychiy V, Kosse S, Ludwig P, Melzer A and Piel A 2005 *J. Phys.: Conf. Ser.* **11** 234–47
[21] Golubnychiy V, Baumgartner H, Bonitz M, Filinov A and Fehske H 2006 *J. Phys. A: Math. Gen.* **39** 4527

[22] Apolinario S W S, Partoens B and Peeters F M 2007 *New J. Phys.* **9** 283
[23] Baumgartner H, Kählert H, Golubnychiy V, Henning C, Käding S, Melzer A and Bonitz M 2007 *Contrib. Plasma Phys.* **47** 281–90
[24] Bonitz M, Block D, Arp O, Golubnychiy V, Baumgartner H, Ludwig P, Piel A and Filinov A 2006 *Phys. Rev. Lett.* **96** 075001
[25] Apolinario S W S 2008 *PhD Thesis* University of Antwerp
[26] Antonova T, Annaratone B M, Goldbeck D D, Yaroshenko V, Thomas H M and Morfill G E 2006 *Phys. Rev. Lett.* **96** 115001
[27] Henning C, Baumgartner H, Piel A, Ludwig P, Golubnychiy V, Bonitz M and Block D 2006 *Phys. Rev.* E **74** 056403
[28] Henning C, Ludwig P, Filinov A, Piel A and Bonitz M 2007 *Phys. Rev.* E **76** 036404
[29] Arp O, Block D, Klindworth M and Piel A 2005 *Phys. Plasmas* **12** 122102
[30] Kirkpatrick S and Gelatt C D 1983 *Science* **220** 671
[31] Hamaguchi S, Farouki R T and Dubin D H E 1997 *Phys. Rev.* E **56** 4671
[32] Totsuji H, Totsuji C, Ogawa T and Tsuruta K 2005 *Phys. Rev.* E **71** 045401
[33] Cioslowski J and Buchowiecki M 2008 *Chem. Phys. Lett.* **456** 146–9
[34] Kamimuraa T, Suga Y and Ishihara O 2007 *Phys. Plasmas* **14** 123706
[35] WalesD J and Doye J P K 1997 *J. Phys. Chem.* A **101** 5111–6
[36] Block D, Käding S, Melzer A, Piel A, Baumgartner H and Bonitz M 2008 *Phys. Plasmas* **15** 040701
Block D, Käding S, Melzer A, Piel A, Baumgartner H and Bonitz M 2008 *Phys. Plasmas* **15** 073710
[37] Kählert H, Ludwig P, Baumgartner H, Bonitz M, Block D, Käding S, Melzer A and Piel A 2008 *Phys. Rev.* E at press (arXiv:0805.3016)
[38] Schiffer J P 2002 *Phys. Rev. Lett.* **88** 205003
[39] Henning C, Fujioka K, Ludwig P, Piel A, Melzer A and Bonitz M 2008 *Phys. Rev. Lett.* **101** 045002